The optical properties of particles deposited on a surface.

Final Technical Report
by
F. Borghese
September 1994

United States Army
European Research Office of the U. S. Army
London - England

Contract no. DAJA45-93-C-0043
Contractor: Prof. V. Grasso
Centro Siciliano per le Ricerche Atmosferiche e di Fisica dell'Ambiente

The optical properties of particles deposited on a surface.

Final Technical Report on Contract DAJA45-93-C-0043

1. Outline of the research.

In recent years the optical properties of particles near or on a plane surface have been the subject of several papers that deal with both the theoretical and the experimental aspects of the problem. This interest from the scientific community can be easily understood because revealing through optical measurements the presence of particles on a surface that is expected to be clean is of great importance both for industry and fo medicine.

Among the theoretical techniques th been proposed to deal with the problem the method of the images prov the most fruitful when the plane surface is a perfectly reflecting one, a dit:on that is met to a high degree of accuracy by many polished metallic sur s. According to the theory of the images the problem of scattering from a particle in the vicinity of a perfectly reflecting plane surface is quite equivalent to the problem of the dependent scattering from the compound object that is composed by the actual particle and by its mirror image when excited by the superposition of the fields that come from the actual source and from its image. Of course, the method of the images is advantageous provided one is able to solve, without undue computational effort, the problem of scattering from the compound scatterer. In fact, the lack of an efficient technique to deal with this problem forced several researchers to solve the problem for limiting cases only, e. g. normal incidence, or through approximations, such as the assumption of smallness of the scattering particle.

2. Method of attack.

The method that we used for our research combines the method of the images with the technique that we developed several years ago to calculate the scattering properties of aggregated spheres. When one assumes that the actual particle is or can be modelled as a cluster of spherical scatterers, the method of the images requires to deal with the properties of a cluster that contains twice as many spheres as the actual object. The fact that the exciting field is the superposition of two plane waves does not introduce any additional difficulty. Furthermore, the presence of the reflecting surface does not prevent us from performing analytical averages over the orientations of the scattering particles. Therefore our approach is suitable to calculate the scattering pattern not only from single spheres and from single aggregates of spheres but also from a dispersion of identical aggregates whose orientations differ only for a rotation around an axis orthogonal to the reflecting surface.

As our approach does not imply any approximation nor limitation both on the direction of incidence and of observation and on the polarization both of the incident and of the scattered field, we were able to calculate the full scattering pattern for a few representative examples of aggregates that are meant to simu-

late the presence of anisotropic particles on the reflecting surface. Moreover, our approach applies also to hemispheres and to aggregated hemispheres with their flat face lying on the surface; this suggests the possibility of simulating the properties of an arbitrarily rough metallic surface.

3. Sketch of the results.

Although both the theory and the main results of our research are fully explained in the enclosed paper, that has been accepted for publication in JOSA A, it may be useful to summarize here the most relevant findings.

For a dispersion of model anisotropic particles on the surface our results show that the anisotropy is not masked by the random orientation of the particles; the anisotropy can be revealed by observing the polarized light that propagates along the reflecting surface at right angles to the plane of incidence.

The need to deal with the compound scatterer (actual particle and its image) persists until the distance between the actual particle and the surface does not exceed $5d$, where d is the linear size of the actual particle (for spheres, d coincides with the diameter).

The approximations that are based on the assumption of smallness of the scattering particles may present severe drawbacks. In fact, although a small particle in the vicinity of the surface is equivalent to the cluster of two identical small particles, the cluster itself may be not small enough to grant the applicability of the Rayleigh approximation.

4. List of publications.

F. Borghese, P. Denti, R. Saija, E. Fucile and O. I. Sindoni, "Optical properties of particles on or near a perfectly reflecting surface," Accepted for publication in J. Opt. Soc. Am. A

5. Partecipants to the research.

F. Borghese, P. Denti, R. Saija and O. I. Sindoni

E. Fucile, who, thak to the work done under the present Contract Gained the degree of Dottore di Ricerca in Fisica (Resarch Doctor in Physics, more or less equivalent to the amlerican Ph. D. in Physics)

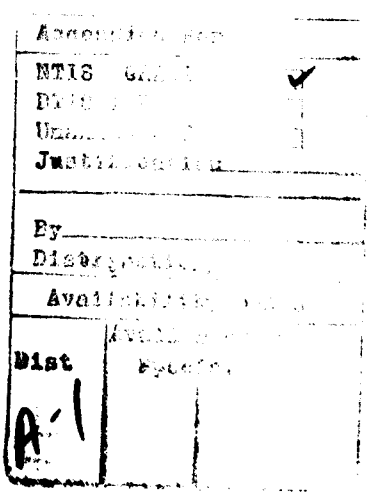

Optical properties of model anisotropic particles on or near a perfectly reflecting surface

F. Borghese, P. Denti, R. Saija
Università di Messina, Istituto di Struttura della Materia
98166 Messina, Italy

E. Fucile
Centro Siciliano per le Ricerche Atmosferiche e di Fisica dell'Ambiente
98166 Messina, Italy

O. I. Sindoni
Edgewood Research Development Engineering Center,
Aberdeen Proving Ground, Md 21010, U. S. A.

In the framework of the image theory the full scattering pattern from model anisotropic particles on a perfectly reflecting surface is calculated for an arbitrary direction of the incident field. The particles on the surface are modelled either as clusters of spherical scatterers or as clusters of hemispheres whose flat face lies on the reflecting surface. Our approach is based on the expansion of all the fields in terms of spherical multipoles whose transformation properties are used to get a compact expression for the scattered intensity both from a single particle as a function of its orientation and from a dispersion of randomly oriented particles. The patterns that were calculated for several model scatterers show some features that may give useful suggestions on the possible anisotropy of actual particles on a reflecting surface.

1. Introduction

The exact solution to the problem of electromagnetic scattering from particles near or on a substrate of general dielectric properties bounded by a plane surface has been worked out for spheres only.[1–4] The literature also reports approximate solutions both for spheres and for particles of general shape that apply e. g. to objects far from the surface or to small objects on the surface itself.[5,6] The need to resort to approximations is not surprising because the simultaneous presence of the closed surface of the particle and of the open plane surface of the substrate complicates the boundary condition problem that one has to solve to get the pattern of the scattered radiation. When the plane surface is perfectly reflecting the image theory allows one to substitute the problem at hand with the equivalent problem of scattering from the object that is composed by the actual scatterer and by its image,[7] but this substitution amounts to an effective simplification only when the dependent scattering from the compound object can be calculated. Actually, in the case of a perfectly reflecting surface an exact solution has been worked out for both spheres[5,8] and cylinders.[9]

In this paper we will resort just to the image theory to calculate the pattern of the scattered radiation from single model anisotropic particles on or near a perfectly reflecting plane as well as the pattern from a dispersion of identical model anisotropic particles, with random orientation, that form a low-density monolayer on or near the surface. The anisotropic particles will be modelled as clusters of spherical scatterers on account that, in the framework of the image theory, the scattering from a single sphere near a perfectly reflecting surface is equivalent to the dependent scattering from the binary cluster that is composed of the actual sphere and of its image, provided the exciting field is the superposition of the fields that come from the actual source and from its image.[8] Thus, if the object in front of the surface is a cluster of spheres, one has to deal with the scattering pattern from a cluster that has twice the spheres than the actual cluster.

The scattering from a cluster of spheres can be calculated with a high degree of precision and without undue computational effort through the technique that we devised a few years ago.[10] We based our approach on the expansion of the incident, of the scattered and of the internal field in terms of spherical multipoles[11–14] and on the imposition of the appropriate boundary conditions at the surface of each one of the spheres in the cluster. The

final equations are affected by no approximation and, in fact, proved to yield results that are in excellent agreement with the available experimental data for single clusters.[15,16] A noticeable feature of our formalism is that, through the use of the transformation properties of the spherical multipoles under rotation, the scattering amplitude of any cluster turns out to be factorized into a part that depends only on the structure and on the orientation of the cluster and into another part that depends only on the polarization and on the direction both of the incident and of the scattered field.[17] On account of this separation the pattern of the scattered radiation from a cluster of arbitrary orientation can be calculated, without undue computational effort, for whatever polarization and direction both of incidence and of observation. Our formalism is also suitable to calculate the scattering pattern from an assembly of identical clusters with random orientation, provided their number density is so low that the multiple scattering processes among different clusters can be neglected. The scattering amplitude depends, indeed, on the orientation of the cluster only through the D-matrices, i. e. through the irreducible representations of the three-dimensional rotation group;[18] therefore, once the scattering amplitude is known for a single orientation, it is also immediately known for any other orientation. Using this dependence of the scattering amplitude on the orientation, the average that must be calculated to get the scattering pattern from the whole assembly can be performed analytically in many cases of interest; even when the average must be performed numerically the computation requires, however, little effort.

In this paper we will use just the formalism that we outlined above[10,17] to calculate the scattered intensity from a dispersion of identical clusters on the reflecting surface; our only assumption is that the actual objects together with their images are still identical to each other and that the orientations of any two clusters differ for a rotation around an axis orthogonal to the reflecting surface. We stress that our procedure does not imply any limitation either on the polarization or on the direction both of the incident and of the observed wave. The same procedure is also applicable to one or more hemispheres whose flat face lies on the surface as these objects, together with their images, form either a single sphere or a cluster of spheres. In this paper we will also deal with the scattering pattern from these objects in order to gain some information on their properties because, in our opinion, a dispersion of hemispheres on a plane surface could be an useful model to simulate the properties of e. g. a rough metallic surface.

2. Theory

A. The incident field and the reflected field

Let us assume that the halfspace $z < 0$ is filled with a perfectly conducting material, such as a metal: the bounding surface $z = 0$ is thus perfectly reflecting. We assume that the incident field is the plane wave

$$\mathbf{E}^{\mathrm{inc}} = E_0 \hat{\mathbf{e}}_I \exp(i\mathbf{k}_I \cdot \mathbf{r})$$

that propagates in the halfspace $z > 0$ of (real) refractive index n with (unit) polarization vector $\hat{\mathbf{e}}_I$ and wavevector $\mathbf{k}_I = nk\hat{\mathbf{k}}_I$; as usual, $k = \omega/c$ and the time dependence $\exp(-i\omega t)$ is omitted throughout. The multipole expansion of the incident field is

$$\mathbf{E}^{\mathrm{inc}} = E_0 \sum_{plm} W^{(p)}_{Ilm} \mathbf{J}^{(p)}_{lm}(nk, \mathbf{r}), \tag{1}$$

where we define the spherical multipoles

$$\mathbf{J}^{(1)}_{lm}(k, \mathbf{r}) = j_l(kr)\mathbf{X}_{lm}(\hat{\mathbf{r}}), \qquad \mathbf{J}^{(2)}_{lm}(k, \mathbf{r}) = \frac{1}{k}\nabla \times \mathbf{J}^{(1)}_{lm}(k, \mathbf{r})$$

whose parity is given by the superscript $p = 1, 2$ that distinguishes the magnetic multipoles ($p = 1$) from the electric ones ($p = 2$); the $\mathbf{X}_{lm}$'s are vector spherical harmonics.[14] In turn the multipole amplitudes W_I are defined as

$$W^{(p)}_{Ilm} = W^{(p)}_{lm}(\hat{\mathbf{e}}_I, \hat{\mathbf{k}}_I),$$

where

$$W_{lm}^{(1)}(\hat{\mathbf{e}},\hat{\mathbf{k}}) = 4\pi i^l \hat{\mathbf{e}} \cdot \mathbf{X}_{lm}^*(\hat{\mathbf{k}}), \qquad W_{lm}^{(2)}(\hat{\mathbf{e}},\hat{\mathbf{k}}) = 4\pi i^{l+1}(\hat{\mathbf{k}} \times \hat{\mathbf{e}}) \cdot \mathbf{X}_{lm}^*(\hat{\mathbf{k}}).$$

The reflected field coincides with the field that comes from the mirror image of the source and has the expansion

$$\mathbf{E}^{ref} = E_0 \sum_{plm} W_{Rlm}^{(p)} \mathbf{J}_{lm}^{(p)}(nk,\mathbf{r}).$$

Of course, the condition of reflection implies that the polarizations of $\mathbf{E}^{inc}$ and $\mathbf{E}^{ref}$ cannot be mutually independent; therefore the relation between them will be presently established. Since the plane $z = 0$ is perfectly reflecting, there is no transmitted field: thus $\mathbf{E}^{inc}$ and $\mathbf{E}^{ref}$ must have the same amplitude as well as the same phase on that plane. Therefore, the boundary conditions at the reflecting surface read

$$(\hat{\mathbf{e}}_I + \hat{\mathbf{e}}_R) \times \hat{\mathbf{n}} = 0, \tag{2}$$

where $\hat{\mathbf{n}}$ is the unit normal to the surface. In order to find the explicit relation between the polarization of the incident and of the reflected wave it is convenient to introduce a basis for the projection of the states of polarization. For the incident wave we introduce the pair of unit vectors $\hat{\mathbf{u}}_{I\parallel}$, that lies in the plane of $\hat{\mathbf{k}}_I$ and of $\hat{\mathbf{n}}$ and is orthogonal to $\hat{\mathbf{k}}_I$, and $\hat{\mathbf{u}}_{I\perp} = \hat{\mathbf{k}}_I \times \hat{\mathbf{u}}_{I\parallel}$; for the reflected wave we define the pair $\hat{\mathbf{u}}_{R\parallel}$ and $\hat{\mathbf{u}}_{R\perp}$ that are orthogonal to $\hat{\mathbf{k}}_R$ and to each other with $\hat{\mathbf{u}}_{R\parallel}$ in the plane of $\hat{\mathbf{k}}_R$ and $\hat{\mathbf{n}}$. By projecting $\hat{\mathbf{e}}_I$ and $\hat{\mathbf{e}}_R$ on the respective basis and imposing the boundary conditions, eq. (2), we get

$$e_{R\parallel} = e_{I\parallel}, \qquad e_{R\perp} = -e_{I\perp}$$

when the polarization is linear. For the case of circular polarization we define the bases

$$\hat{\mathbf{u}}_{I\mp} = \frac{1}{\sqrt{2}}(\hat{\mathbf{u}}_{I\parallel} \mp i\hat{\mathbf{u}}_{I\perp}), \quad \hat{\mathbf{u}}_{R\mp} = \frac{1}{\sqrt{2}}(\hat{\mathbf{u}}_{R\parallel} \mp i\hat{\mathbf{u}}_{R\perp}),$$

and with the same procedure we get

$$e_{R-} = e_{I+}, \qquad e_{R+} = e_{I-}.$$

Although the field that actually excites the particles is $\mathbf{E}^{exc} = \mathbf{E}^{inc} + \mathbf{E}^{ref}$, the relations above allow us to refer to the direction of incidence and to the polarization of the incident field only.

B. The scattered field

The field that is scattered by the compound object that includes the actual particle and its mirror image can be expanded as

$$\mathbf{E}^{sca} = E_0 \sum_{plm} A_{lm}^{(p)} \mathbf{H}_{lm}^{(p)}(nk,\mathbf{r}), \tag{3}$$

where the multipole fields $\mathbf{H}_{lm}^{(p)}$'s are identical to the $\mathbf{J}_{lm}^{(p)}$'s except for the substitution of the spherical Hankel functions $h_l^{(1)}(kr)$ to the spherical Bessel functions $j_l(kr)$. The amplitudes $A_{lm}^{(p)}$ are related to the amplitudes of the exciting field $\mathbf{E}^{exc}$ through the equation

$$A_{lm}^{(p)} = -\sum_{p'l'm'} S_{lm,l'm'}^{(p,p')} W_{El'm'}^{(p')}, \tag{4}$$

where

$$W_{El'm'}^{(p')} = W_{Il'm'}^{(p')} + W_{Rl'm'}^{(p')}.$$

The matrix S, of elements $S^{(p,p')}_{lm,l'm'}$, is the so called transition matrix[19] and contains all the structural information on the aggregate composed of the particle and of its image. The form of eq. (4) is essential to perform the angular analysis of the scattered radiation, as in this equation the structural information is factorized with respect to the angular information. In other words, S depends on the geometry, on the orientation and on the scattering power of the particle whereas all the information on the direction and on the polarization of the incident wave is contained in the W_E's.

Let us now recall that the particles that we deal with in this paper together with their image always form a cluster of spheres; therefore their S-matrix can be evaluated through the technique that we devised several years ago to describe the scattering properties of aggregated spheres. The complete theory has been published elsewhere[10] so that, in Appendix A, we report only the guidelines of our procedure for the calculation of S. This matrix is related to the matrix $\mathcal{M}^{-1}$ that is the inverse of the matrix $\mathcal{M}$ that expresses the boundary conditions at the surface of each one of the spheres in terms of multipole fields.[10] The matrix $\mathcal{M}$ accounts for the fact that the incident field on each one of the spheres is the superposition of $\mathbf{E}^{exc}$ and of the fields that have already been scattered by all the other spheres in the aggregate. In other words the field scattered by the whole aggregate is calculated through a dependent scattering approach. For an aggregate of N spheres with no particular symmetry the order of $\mathcal{M}$ is $d_{\mathcal{M}} = 2NL_{\mathcal{M}}(L_{\mathcal{M}}+2)$, where $L_{\mathcal{M}}$ is the maximum value of l that must be retained into the expansions eq. (1) and (3) to get fairly convergent results for the scattered field. Therefore, $\mathcal{M}$ can become rather big thus requiring a long computer time for its inversion; actually, the calculation of $\mathcal{M}^{-1}$ is responsible for the most part of the calculations that are needed to get the scattered field. The use of group theory, however, may help to reduce the computational effort through the exploitation of the symmetry properties of the scatterer.[20,21] In this respect, it is worth recalling that our compound scatterers (actual object and its image) do have at least the reflection symmetry with respect to the plane of the substrate. Furthermore, if the compound scatterers have also the cylindrical symmetry around an axis orthogonal to the surface, the direct use of the machinery of group theory is not necessary, because the choice of the cylindrical axis as the z axis produces an automatic factorization of the $\mathcal{M}$ matrix with respect to the index m. In this case the highest order of the matrices to be inverted is $d_{\mathcal{M}} = 2NL_{\mathcal{M}}$ only.

C. The scattered intensity

The relevant quantity is the matrix $I_{\eta\eta'} = E^{sca}_{\eta\eta'} * E^{sca}_{\eta\eta'}$; the indices η and η' refer to the polarization of the scattered and of the incident field, respectively. The scattered field from a particle at the origin of the frame of reference can be written as

$$E^{sca}_{\eta\eta'} = E_0 \frac{\exp(ikr)}{r} f_{\eta\eta'}$$

provided r is large, so that

$$I_{\eta\eta'} = \left| \frac{E_0}{r} f_{\eta\eta'} \right|^2,$$

where the $f_{\eta\eta'}$ are the elements of the normalized scattering amplitude[14] that are known to depend both on the incident and on the scattered wavevector as well as on the orientation of the particle with respect to a frame of reference fixed in the laboratory. Of course, the scattering amplitude that we must consider here is that of the compound scatterer that is composed by the object in front of the surface and by its mirror image. The $f_{\eta\eta'}$ are related to the elements of the transition matrix through the equation[17]

$$f_{\eta\eta'} = \frac{i}{4\pi nk} \sum_{plm} \sum_{p'l'm'} W^{(p)*}_{S\,\eta lm} S^{(p,p')}_{lm,l'm'} W^{(p')}_{E\,\eta' l'm'} \tag{5}$$

with

$$W^{(p)}_{S\,\eta lm} = W^{(p)}_{lm}(\hat{\mathbf{e}}_S, \hat{\mathbf{k}}_S),$$

where $\hat{\mathbf{e}}_S$ and $\hat{\mathbf{k}}_S$ are the polarization vector and the direction of observation of the scattered field, respectively. If one has to calculate the scattering pattern from a single cluster in the vicinity of the reflecting surface, eq. (5) is

quite efficient as its form shows that, once the S-matrix is known, the scattered intensity can be calculated without undue computational effort for any $\hat{\mathbf{k}}_I$ and $\hat{\mathbf{k}}_S$.

When one is interested in the pattern of the scattered radiation from an assembly of identical scatterers in front of the surface, the distribution of their orientations must be taken into account. This can be done by associating to each cluster a local system of axes chosen so that when two clusters are superposed their respective local axes coincide. As explained elsewhere in full detail,[17] the scattering amplitude of a cluster of known orientation is given by

$$f_{\eta\eta'} = \frac{i}{4\pi nk} \sum_{plm} \sum_{p'l'm'} \sum_{\mu\mu'} W^{(p)*}_{S\eta lm}\, D^{(l)*}_{\mu m}(\Theta)\, \overline{S}^{(p,p')}_{l\mu,l'\mu'}\, D^{(l')}_{\mu' m'}(\Theta)\, W^{(p')}_{E\eta' l' m'}, \tag{6}$$

where $\Theta \equiv (\alpha, \beta, \gamma)$ is a shorthand for the three Euler angles[12] that characterize the orientation of the local frame with respect to the laboratory frame. In eq. (6) both $W^{(p)*}_{S\eta lm}$ and $W^{(p')}_{E\eta' l' m'}$ are given in the laboratory frame whereas the elements of the transition matrix, $\overline{S}^{(p,p')}_{l\mu,l'\mu'}$, are calculated in the local frame and are thus independent of the orientation of the scatterer; the D's, in turn, are the irreducible representations of the rotation group,[11,18] i. e. the matrices that transform the laboratory frame into the local frame. Equation (6) shows that, even when dealing with an assembly of identical scatterers, we need to calculate the transition matrix only once.

We have now all the ingredients that are necessary to calculate the scattered intensity from an assembly of identical clusters in the vicinity of the reflecting surface. It is to be stressed, however, that the applicability of the method of the images requires that we consider a monolayer of clusters that are so arranged that the centers of the corresponding spheres in different clusters have the same distance from the surface. A moment's thought will convince the reader that this condition implies that all the compound scatterers that are composed by the actual objects and by their respective images are identical to each other and that the orientations of any two of them differ for a rotation around an axis that is perpendicular to the surface. With this in mind we can write the total scattered intensity as

$$\overline{I}_{\eta\eta'} = \left(\sum_{\nu} E^{*}_{\nu\,\eta\eta'} \right) \left(\sum_{\nu'} E_{\nu'\,\eta\eta'} \right) = N \langle |E_{\eta\eta'}(\mathbf{R}, \Theta)|^2 \rangle + (N^2 - N) \langle E^{*}_{\eta\eta'}(\mathbf{R}, \Theta) E_{\eta\eta'}(\mathbf{R}', \Theta') \rangle,$$

where ν and ν' are particle indexes, N is the number of the particles on the reflecting surface, $E_{\eta\eta'}(\mathbf{R}, \Theta)$ is the scattered field from a particle at the position $\mathbf{R}$ with orientation Θ, and the brackets denote the ensemble average over both the position and the orientation of the particles. The first term on the right-hand side, the so called self term, contributes to the scattered intensity for any angle of observation. Even the second term, that is a two-body term, may become important for nonrandom distributions of the scatterers, but, when they are randomly distributed upon the surface, it does contribute in the direction of reflection only.[22] Ultimately, as in this paper we deal just with monolayers of randomly distributed scatterers, we will outright disregard the two-body term so that $\overline{I}_{\eta\eta'}$ reduces to

$$\overline{I}_{\eta\eta'} = N \langle I_{\eta\eta'} \rangle = N \int I_{\eta\eta'}(\mathbf{R}, \Theta) w(\mathbf{R}, \Theta)\, \mathrm{d}\mathbf{R}\, \mathrm{d}\Theta,$$

where $w(\mathbf{R}, \Theta)$ is the normalized density distribution function with respect to the position of the particles and their angular orientation. Since we assume that there is no correlation between the position and the orientation of the scatterers w can be factorized as $w(\mathbf{R}, \Theta) = w_{\mathbf{R}}(\mathbf{R}) w_{\Theta}(\Theta)$; furthermore the distance of observation is assumed, as usual, to be very large with respect to the size of the reflecting surface, so that we can put $\mathbf{R} = 0$ and write

$$\begin{aligned} \langle I_{\eta\eta'} \rangle &\approx \int I_{\eta\eta'}(\mathbf{R}, \Theta) w_{\mathbf{R}}(\mathbf{R}) w_{\Theta}(\Theta)\, \mathrm{d}\mathbf{R}\, \mathrm{d}\Theta \approx \int w_{\mathbf{R}}(\mathbf{R})\, \mathrm{d}\mathbf{R} \int I_{\eta\eta'}(0, \Theta) w_{\Theta}(\Theta)\, \mathrm{d}\Theta \\ &= \int I_{\eta\eta'}(0, \Theta) w_{\Theta}(\Theta)\, \mathrm{d}\Theta, \end{aligned}$$

on account that

$$\int w_{\mathbf{R}}(\mathbf{R})\, \mathrm{d}\mathbf{R} = 1.$$

The orientation of any two clusters differs only by a rotation around an axis that is orthogonal to the surface; thus, we choose the z axis of the local reference frame that we attached to each cluster to coincide with that axis, $\beta = \gamma = 0$, and the average involves the Euler angle α only. Now,[12]

$$D^{(l)}_{\mu m}(\alpha, 0, 0) = \exp(-i\mu\alpha)\delta_{\mu m},$$

so that eq. (6) reads

$$f_{\eta\eta'} = \frac{i}{4\pi nk} \sum_{plm} \sum_{p'l'm'} W^{(p)*}_{S\eta lm} \exp(im\alpha)\, \overline{S}^{(p,p')}_{lm,l'm'} \exp(-im'\alpha)\, W^{(p')}_{E\eta' l'm'}.$$

Then, the total scattered intensity is

$$\overline{I}_{\eta\eta'} = \frac{N}{16\pi^2 k^2 r^2} \left|\frac{E_0}{n}\right|^2 \sum_{mm'} \sum_{m''m'''} F^*_{\eta\eta' mm'} F_{\eta\eta' m''m'''} \mathcal{I}_{m-m'-m''+m'''}, \tag{7}$$

where

$$F_{\eta\eta' mm'} = \sum_{pl} \sum_{p'l'} W^{(p)*}_{S\eta lm}\, \overline{S}^{(p,p')}_{lm,l'm'}\, W^{(p')}_{E\eta' l'm'} \tag{8}$$

and

$$\mathcal{I}_\mu = \int_0^{2\pi} \exp(-i\alpha\mu) w(\alpha) d\alpha,$$

where in turn

$$w(\alpha) = w_\Theta(\alpha, \beta = 0, \gamma = 0).$$

Equation (7) gives the scattered intensity for a general orientational distribution of the scatterers, i. e. for a general $w(\alpha)$. In particular, if $w(\alpha) = 1/2\pi$, i. e. when the clusters are randomly oriented, $\mathcal{I}_\mu = \delta_{\mu,0}$; this implies that the sums in eq. (7) are subject to the constraint $m - m' - m'' + m''' = 0$.

The average over the orientations is, of course, not necessary and is actually not performed in two important cases: when all the compound scatterers are oriented alike or when they have cylindrical symmetry around an axis perpendicular to the surface. The latter case occurs when the centers of all the spheres that form a cluster lie on a straight line that is perpendicular to the surface. However, even in these two special cases our orientational averaging procedure yields the correct results as we will show presently. When all the clusters are oriented alike, $\overline{S}$ can be calculated with respect to a local reference frame whose axes are parallel to those of the laboratory frame; as a consequence $w(\alpha) = \delta(\alpha)$, where δ is the Dirac delta function, and $\mathcal{I}_\mu = 1$, so that eq. (7) becomes

$$\overline{I}_{\eta\eta'} = \frac{N}{16\pi^2 k^2 r^2} \left|\frac{E_0}{n}\right|^2 \sum_{mm'} \sum_{m''m'''} F^*_{\eta\eta' mm'} F_{\eta\eta' m''m'''}.$$

If the clusters have cylindrical symmetry, the elements $\overline{S}^{(p,p')}_{lm,l'm'}$ do not vanish for $m = m'$ only,[19] and the same holds true for $F_{\eta\eta' mm'}$, eq.(8), because we just chose the cylindrical axis as the z axis of the local frame; consequently, eq. (7) simplifies to

$$\overline{I}_{\eta\eta'} = \frac{N}{16\pi^2 k^2 r^2} \left|\frac{E_0}{n}\right|^2 \sum_{mm''} F^*_{\eta\eta' mm} F_{\eta\eta' m''m''},$$

on account that $\mathcal{I}_{m-m'-m''+m'''} = \mathcal{I}_0 = 1$ according to its definition. Thus even in the above mentioned special cases our orientation averaging procedure works properly and yields the trivial result that the total scattered intensity equals N times the intensity that is scattered by an individual particle[23,13].

3. Results and discussion

The theory that we described in the preceding sections has been tested against the results reported by Johnson for a single sphere near or in contact with the reflecting surface. Actually, we were able to reproduce with the highest accuracy the results that Johnson reports in Figs. 7–10 of his paper.[8] However, we are not restricted to normal incidence so that we are able to calculate the full pattern of the scattered intensity at any incidence not only for a single sphere on the reflecting surface but also for some representative anisotropic model particles. In fact, we performed our calculations also for a cluster of two identical and mutually contacting spheres lying on the surface as well as for clusters of two identical mutually contacting hemispheres and for linear chains of four identical hemispheres — the neighbouring hemispheres are in contact with each other — with their flat face lying on the reflecting surface. With the exception of the case of a single sphere, almost all the patterns that we report refer to a dispersion of identical objects whose orientations are randomly distributed as explained in Subsection 2C. In our calculations we assumed that the medium that fills the accessible half-space is the vacuum ($n = 1$) and that the wavelength of the incident radiation is $\lambda = 628.3\,\mathrm{nm}$; the refractive index of both the spheres and the hemispheres is $n_0 = 3$ while the radius both of the single sphere and of the hemispheres that form a binary cluster was chosen to be $b_s = 126.0\,\mathrm{nm}$; in turn the radius both of the spheres that form the binary cluster and of the hemispheres that form the four-hemispheres chain is $b_h = 100.0\,\mathrm{nm}$. This choice of the radii is not casual as it makes the total volume of all the clusters, either of spheres or of hemispheres, equal to the volume of the single sphere. In fact, since we are mainly interested in the effects of the anisotropy, we found it convenient, according to our previous experience,[24] to investigate objects with a different geometry but containing the same quantity of refractive material. The size parameter of the single sphere turns out to be $x_s = kb_s = 1.26$ whereas the size parameter of the spheres that form the binary clusters is $x_h = kb_h = 1.0$. As a result, the maximum value of l that we had to include into the multipole expansions, eqs. (1) and (3), was $L_M = 8$ for the single sphere, $L_M = 9$ for the two-hemispheres clusters and $L_M = 10$ both for the two-spheres and the four-hemispheres clusters in order to achieve the convergence to four significant digits: this convergence criterion is, of course, more strict that required for an accurate display of our results. The need to use so large a value of L_M even for the single sphere is due to the fact that our calculations do not actually deal with a single sphere but rather with the two-sphere cluster that is composed by the actual sphere and by its image. Now, according to Waterman,[19] we define the size parameter, x, of a non-spherical object as the size parameter of the smallest sphere that may contain the object itself. Accordingly, for the single sphere we have $x = 2.52$ and even larger values for the other clusters that we consider in this paper. If one also adds that the refractive index is $n_0 = 3$ the values of L_M that we quoted above can in no way be considered too large.

Before discussing our results let us recall that the theory of the preceding sections has been set up on the assumption that the z axis is orthogonal to the reflecting surface. This choice is hardly compulsory but, for cylindrically-symmetric particles, it yields the automatic factorization of the matrix $\mathcal{M}$ as explained at the end of Subsection 2C. We also stress that, according to the set up of the theory, the polar angles of the direction of observation should be in the range $0 \leq \varphi_S \leq 360°$ and $0 \leq \vartheta_S \leq 90°$. We preferred, instead, to display our results with respect to the frame of reference that is sketched in Fig. 1: the reflecting surface coincides with the xz plane and the y axis is thus orthogonal to the surface and directed towards the accessible halfspace. Accordingly, the scattering pattern is reported for $0 \leq \varphi_S \leq 180°$ and $0 \leq \vartheta_S \leq 180°$. Since the scattering pattern depends on the direction of incidence, the latter need to be specified. Now, according to eq. (6), once the matrix S is known, the generation of the scattering pattern for several values of ϑ_I and φ_I is a fast and low-cost operation that produces a large amount of data, however. Therefore we resolved to report all the scattering patterns for a single direction of incidence only. This direction, that in Fig. 1 is indicated by an arrow, was chosen to form an angle of 45° with the normal to the surface and has thus $\vartheta_I = 90°$ and $\varphi_I = 225°$.

We also chose to not refer the state of polarization to a pair of basis vectors that are parallel and orthogonal to the scattering plane, i. e. to the plane of $\mathbf{k}_I$ and $\mathbf{k}_S$; we preferred instead to project the polarization vector along the pair of unit vectors $\hat{\vartheta}$ and $\hat{\varphi}$ that are tangent to the the meridians and to the parallels, respectively, of the big sphere that is depicted in Fig. 1. Of course, on account of this choice, the appearance of cross-polarization effects is expected even when the scatterer is a single sphere.

The quantity that we report in Figs. 2–4 as a function of ϑ_S and φ_S is $r^2 I_{\eta\eta'}/I_0$ for the single particles and $r^2\langle I_{\eta\eta'}\rangle/I_0$ for the dispersions, where r is the distance of observation, I_0 the incident intensity, $I_{\eta\eta'}$ is the observed intensity, $\langle I_{\eta\eta'}\rangle$ is the orientationally-averaged observed intensity; the indices η and η' indicate the polarization of the observed and of the incident field, respectively, and take on the symbolic values ϑ and φ to denote polarization

along the meridians (ϑ-polarization) and along the parallels (φ-polarization), respectively. It should also be noticed that even when ϑ_S reaches its limiting values, $\vartheta_S = 0°$ and $\vartheta_S = 180°$, the angle φ_S is still well defined as this angle characterizes an observation with a well defined choice of the polarization, e. g. along the meridians. Thus, the limiting curves of our patterns ($\vartheta_S = 0°$ and $\vartheta_S = 180°$) describe the observation of the scattered beam that propagates along the reflecting surface at right angles to the plane of incidence with a polarization that depends on φ_S: so, for the ϑ-polarized component of the scattered wave, when $\varphi_S = 90°$, $\mathbf{E}^{sca}$ is orthogonal to the surface, whereas when $\varphi_S = 0°$ or $\varphi_S = 180°$, $\mathbf{E}^{sca}$ is parallel to the reflecting surface and thus, as a direct consequence of the boundary conditions, the scattered intensity must vanish; for the φ-polarized component of the scattered wave, when $\varphi_S = 0°$ or $\varphi_S = 180°$, $\mathbf{E}^{sca}$ is orthogonal to the surface whereas, when $\varphi_S = 90°$, $\mathbf{E}^{sca}$ is parallel to the reflecting surface and thus the scattered intensity must again vanish. Since, for any given polarization, the four extreme vertices of the pattern correspond to the same physical situation, the scattered intensity must have the same value at all these extreme points; a further consequence is that e. g. $I_{\varphi\varphi}(\vartheta_S = 0°, \varphi_S = 0°) = I_{\vartheta\varphi}(\vartheta_S = 0°, \varphi_S = 90°)$.

All these features can be seen in Figs. 2-4 that report the results of our calculations. In particular, Fig. 2 reports the scattering pattern (a) for a single sphere on the surface, (b) for a dispersion of randomly oriented clusters of two mutually contacting spheres on the surface, (c) for a dispersion of randomly oriented linear chains of four hemispheres and (d) for a linear chain of four hemispheres along the z axis; the flat face of all the hemispheres lies on the reflecting surface. The incident field is φ-polarized and the φ-polarized component of the scattered wave is considered. We first remark that the pattern for a single sphere in Fig. 2(a) shows only a symmetry of reflection in the plane of incidence. Therefore, even for such a cylindrically symmetric object all the directions of scattering must be considered when the incidence is not normal to the reflecting plane. In all the four patterns in Fig. 2 we notice the presence of a strong scattered beam that propagates along the reflecting surface in the forward direction ($\vartheta_S = 90°, \varphi_S = 180°$). We also notice the two wings in the pattern from the linear chain of four-hemispheres in Fig. 2(d). The comparison with the orientationally averaged pattern in Fig. 2(c) suggests that the observed wings are a result of the particular orientation of the scatterers. Let us now consider the limiting curves at $\vartheta_S = 0°$ and $\vartheta_S = 180°$. It is quite evident that these curves are almost flat for all the clusters but are in no way flat for the single sphere. This suggests that the observation of the scattered light that propagates along the reflecting surface may yield useful information on the shape of the scattering particles.

This is confirmed by the patterns in Fig. 3 that report our results (a) for a single sphere and for the assemblies (b) of randomly oriented two-spheres clusters, (c) two-hemispheres clusters and (d) four-hemispheres linear chains. The incident wave is ϑ-polarized and the φ-polarized component of the scattered wave is considered, so that all the patterns describe cross-polarization effects. Let us remark first that the patterns in (a) and (b), that refer to a single sphere and to the two-sphere clusters, present a couple of peaks for non-limiting values of ϑ_S and φ_S: such peaks are not present in the patterns in (c) and (d), that refer to the two-hemispheres and to the four-hemispheres clusters. Furthermore, the patterns for all the clusters, either of spheres and of hemispheres reach their maximum value at the four vertices ($\vartheta_S = 0°, 180°$ and $\varphi_S = 0°, 180°$): this is not the case for the single sphere in (a). The differences of the patterns of the single sphere and of the clusters can be attributed on one hand to the cylindrical symmetry of the single sphere and on the other hand to the anisotropy of the clusters in spite of their random orientation. In other words, the process of averaging does not cancel the effects that are due to the anisotropy of the scatterers. The patterns in Fig. 3 suggest that the effects of the anisotropy are still visible provided that the observation is made with the appropriate polarization.

In Fig. 4 we report the patterns for the same objects that we considered in Fig. 3; the only difference is the choice of the polarization, i. e. the incident wave is φ-polarized and the ϑ-polarized component of the scattered wave is considered. The patterns in (a) and (c), that refer to the single sphere and to the two-hemispheres clusters, show a strong similarity; such a similarity is also shown by the patterns in (b) and (d) that refer to the two-spheres and to the four-hemispheres, respectively. Thus, the general structure of the patterns seems to be related to the number of the spheres that compose the actual scatterers, provided that two hemispheres are counted as one sphere. In this respect we recall that all the scatterers that we investigate in this paper have the same volume.

We do not report any result for the case in which both the incident and the scattered wave are considered to be ϑ-polarized: these patterns do not add in fact any information worth of a separate comment.

4. Conclusions

The results that we reported in the Section 3 suggest a number of considerations both on the applicability of the small particle approximation to the problem at hand and to the ability of our approach to yield useful information for the interpretation of the experimental data.

In the present problem the range of applicability of the Rayleigh scattering approximation (RSA) is even more restricted than in the case of the isolated particles. The use of the theory of the images, indeed, implies that one has to deal with the compound scatterer that is composed by the actual particle and by its mirror image. According to the definition that we quoted in the preceding section,[19] the effective size parameter of such a compound object is larger than the size parameter of the actual scatterer. Of course, if the actual particle is not in contact with the reflecting surface the effective size parameter is bound to increase. Obviously, the RSA is in no way applicable to the scatterers that we consider in this paper both because the size parameter of each component sphere (and of each hemisphere too) is not small and because the refractive index itself is not close to unity. In this respect we recall that we had to consider multipole fields up to $L_M = 10$, in contrast to the RSA that amounts to consider the dipole field only, i. e. $L_M = 1$.

The approach that we used in this paper has been designed just to deal with the scattering properties of anisotropic particles without resorting to any approximation except for the truncation of the multipole expansions whose effect can easily be checked, however. The usefulness of our approach stems from its generality that, in turn, derives from the transformation properties under rotation of the spherical multipole fields and of the transition matrix. As a result, we were able to calculate with a limited computational effort the scattered intensity from assemblies of randomly oriented anisotropic scatterers on the reflecting surface.

The results of our calculations, in particular the results in Figs. 2 and 3, show that the scattering pattern of our model anisotropic scatterers are remarkably different from those of the spherical particles. Therefore, provided this behavior pertains also to more general anisotropic scatterers than the model scatterers that we considered so far, a polarization analysis of the grazing scattered intensity could yield useful information on the possible anisotropy of the particles on the surface.

Appendix A: Scattering from a cluster of spheres

We consider a cluster of N spheres of radius b_α and (possibly complex) refractive index n_α whose centers lie at $\mathbf{R}_\alpha$; the cluster is assumed to be embedded into a homogeneous medium of refractive index n. The incident field, that we assume to be the plane wave whose multipole expansion is given by eq. (1), excites within each sphere the internal field

$$\mathbf{E}^{int}(\mathbf{r}_\alpha) = \sum_{plm} \mathcal{C}^{(p)}_{\alpha lm}\, \mathbf{J}^{(p)}_{lm}(n_\alpha k, \mathbf{r}_\alpha),$$

where $\mathbf{r}_\alpha = \mathbf{r} - \mathbf{R}_\alpha$. By writing the scattered field as a superposition of the fields that are scattered by the single spheres,

$$\mathbf{E}^{sca} = \sum_{\alpha} \sum_{plm} \mathcal{A}^{(p)}_{\alpha lm}\, \mathbf{H}^{(p)}_{lm}(nk, \mathbf{r}_\alpha),$$

the unknown amplitudes $\mathcal{A}^{(p)}_{\alpha lm}$ can be calculated by imposing the boundary conditions across the surface of each one of the spheres in the cluster. In this respect we notice that the scattered field is written in terms of multipole fields that are referred to different origins whereas the incident field is written in terms of multipoles that are referred to the origin of the frame of reference. Therefore, before the boundary conditions are applied we have to use an appropriate addition theorem to refer all the multipole fields to the same origin.[25] For the incident plane wave, e. g., this theorem yields

$$\mathbf{E}^{inc} = \sum_{lm} \mathcal{W}^{(p)}_{\alpha lm} \mathbf{J}^{(p)}_{lm}(nk, \mathbf{r}_\alpha),$$

where

$$\mathcal{W}_{\alpha lm}^{(p)} = \sum_{p'l'm'} \mathcal{J}_{\alpha lm,l'm'}^{(p,p')} \mathcal{U}_{l'm'}^{(p')} \tag{A1}$$

The quantities $\mathcal{J}_{\alpha lm,l'm'}^{(p,p')}$ are the elements of the matrix that performs the transfer of origin of the multipole fields from the unique origin at $\mathbf{R}_0$ to $\mathbf{R}_\alpha$; of course, in the present case the unique origin $\mathbf{R}_0$ coincides with the origin of the reference frame, so that $\mathbf{R}_0 = 0$. We have

$$\mathcal{J}_{\alpha lm,l'm'}^{(p,p')} = \left[\delta_{pp'} - i\sqrt{\frac{2l+1}{l}}(1-\delta_{pp'})\right] \sum_{\mu} C(1, l+1-\delta_{pp'}, l; -\mu, m+\mu) \times$$

$$\times G_{l+1-\delta_{pp'},m+\mu,l',m'+\mu}(K, \mathbf{R}_{\alpha 0}) C(1, l', l'; -\mu, m'+\mu),$$

where $\mathbf{R}_{\alpha 0} = \mathbf{R}_0 - \mathbf{R}_\alpha$ and

$$G_{lm,l'm'}(K, \mathbf{R}_\alpha) = 4\pi \sum_{\lambda} i^{l-l'-\lambda} \mathcal{I}_\lambda(l', m'; l, m)\, j_\lambda(KR) Y_{\lambda,m-m'}^*(\hat{\mathbf{R}}_\alpha). \tag{A2}$$

In the preceding equations the C's are the Clebsch-Gordan coefficients and the quantities $\mathcal{I}_\lambda$ are the Gaunt integrals[12] that are defined as

$$\mathcal{I}_\lambda(l', m'; l, m) = \int Y_{l'm'}^* Y_{lm} Y_{\lambda,m'-m}\, d\Omega$$

$$= \sqrt{\frac{(2\lambda+1)(2l+1)}{1\pi(2l'+1)}}\, C(l, \lambda, l'; 0, 0) C(l, \lambda, l'; m, m'-m).$$

We will also need the inverse transfer from $\mathbf{R}_\alpha$ to $\mathbf{R}_0$ in order to get the scattered field in terms of multipoles referred to an unique origin. This transfer is effected by a matrix whose elements, $\mathcal{J}_{lm,\alpha l'm'}^{(p,p')}$, are identical to the elements $\mathcal{J}_{\alpha lm,l'm'}^{(p,p')}$ above except that in G one must substitute $\mathbf{R}_{0\alpha}$ for $\mathbf{R}_{\alpha 0}$.

Anyway, once the incident and the scattered field are expressed in terms of multipoles referred in turn to each one of the sites of the cluster and the boundary conditions are imposed, one gets, for each p, α, l and m, four equations among which the internal amplitudes $\mathcal{C}_{\alpha lm}^{(p)}$ can be eliminated. As a result, the scattered amplitudes $\mathcal{A}_{\alpha lm}^{(p)}$ turn out to be the solution of the system of linear non-homogeneous equations

$$\mathcal{M}\mathcal{A} = -\mathcal{W}, \tag{A3}$$

where $\mathcal{M} = \mathcal{R}^{-1} + \mathcal{H}$ and $\mathcal{A}$ and $\mathcal{W}$ are the one-column vectors of the amplitudes $\mathcal{A}_{\alpha lm}^{(p)}$ and $\mathcal{W}_{\alpha lm}^{(p)}$, respectively. $\mathcal{R}$ is a diagonal matrix of elements

$$\mathcal{R}_{\alpha lm,\alpha' l'm'}^{(p,p')} = \delta_{pp'}\delta_{ll'}\delta_{mm'}\delta_{\alpha\alpha'} R_{\alpha l}^{(p)}$$

with

$$R_{\alpha l}^{(p)} = \frac{(1+\overline{n}_\alpha\delta_{p1}) u_l(n_\alpha k b_\alpha) u_l'(nkb_\alpha) - (1+\overline{n}_\alpha\delta_{p2}) u_l'(n_\alpha k b_\alpha) u_l(nk_\alpha)}{(1+\overline{n}_\alpha\delta_{p1}) u_l(n_\alpha k b_\alpha) w_l'(nkb_\alpha) - (1+\overline{n}_\alpha\delta_{p2}) u_l'(n_\alpha k b_\alpha) w_l(nkb_\alpha)},$$

where

$$\overline{n}_\alpha = \frac{n}{n_\alpha} - 1, \quad u_l(x) = x j_l(x), \quad w_l(x) = x h_l^{(1)}(x).$$

$R_{\alpha l}^{(1)}$ and $R_{\alpha l}^{(2)}$ coincide with the Mie coefficients b_l and a_l, respectively, for the scattering by a homogeneous sphere of radius b_α and refractive index n_α embedded in a homogeneous medium of refractive index n. The last matrix that we need to define is $\mathcal{H}$ whose elements are

$$\mathcal{H}^{(p,p')}_{\alpha lm,\alpha' l'm'} = (1-\delta_{\alpha\alpha'})\left[\delta_{pp'} - i\sqrt{\frac{2l+1}{l}}(1-\delta_{pp'})\right] \times$$

$$\sum_{\mu} C(1,l+1-\delta_{pp'},l;-\mu,m+\mu) G_{l+1-\delta_{pp'},m+\mu,l',m'+\mu}(K,\mathbf{R}_{\alpha\alpha'}) C(1,l',l';-\mu,m'+\mu),$$

where $G_{lm,l'm'}(K,\mathbf{R}_{\alpha\alpha'})$ is still given by eq. (A2) except for the substitution of $h^{(1)}_{\lambda}$ to j_{λ} and $\mathbf{R}_{\alpha\alpha'} = \mathbf{R}_{\alpha'} - \mathbf{R}_{\alpha}$.

The formal solution of eq. (A3) is

$$\mathcal{A} = -\mathcal{M}^{-1}\mathcal{W}$$

i. e.

$$\mathcal{A}^{(p)}_{\alpha lm} = -\sum_{\alpha'}\sum_{p'l'm'} [\mathcal{M}^{-1}]^{(p,p')}_{\alpha lm,\alpha' l'm'} \mathcal{W}^{(p')}_{\alpha' l'm'}.$$

This equation is rather similar to eq. (4) but we are prevented to identify $\mathcal{M}^{-1}$ with S by the fact that both the $\mathcal{A}$'s and the $\mathcal{W}$'s are the amplitudes of multipoles that are referred to different origins. However, multiplication of the preceding equation by $\mathcal{J}^{(q,p)}_{LM,\alpha lm}$ and summation over α, p, l and m, after substitution for the $\mathcal{W}$'s of their expression in eq. (A1) yields

$$A^{(p)}_{lm} = \sum_{\alpha'}\sum_{p'l'm'} \mathcal{J}^{(p,p')}_{lm,\alpha' l'm'} \mathcal{A}^{(p')}_{\alpha' l'm'},$$

and, ultimately,

$$S^{(p,p')}_{lm,l'm'} = \sum_{\alpha\alpha'}\sum_{qLM}\sum_{q'L'M'} \mathcal{J}^{(p,q)}_{lm,\alpha LM} [\mathcal{M}^{-1}]^{(q,q')}_{\alpha LM,\alpha' L'M'} \mathcal{J}^{(q',p')}_{\alpha' L'M',l'm'}.$$

Appendix: ACKNOWLEDGMENTS

This paper is based on work supported in part by the U. S. Army European Research Office through contract DAJA45-93-C-0043.

1. T. Takemori, M. Inoue and K. Ohtaka, "Optical response of a sphere coupled to a metal substrate," J. Phys. Soc. Jpn. **56**, 1587–1602 (1987).
2. P. A. Bobbert and J. Vlieger, "Light scattering by a sphere on a substrate," Physica **137 A**, 209–242 (1986).
3. P. A. Bobbert, J. Vlieger and R. Greef, "Light reflection from a substrate sparsely seeded with spheres. Comparison with ellipsometric experiment," Physica **137A**, 243–257 (1986).
4. G. Bosi, "Retarded treatment of substrate-related effects on granular films," Physica A **100**, 375–392 (1992).
5. G. Videen, "Light scattering from a sphere on or near a surface," J. Opt. Soc. Am. A **8**, 483–489 (1991); errata, J. Opt. Soc. Am. A **9**, 844–845 (1992).
6. I. V. Lindell, A. H. Sihvola, K. O. Muinonen and P. Barber "Scattering by a small object close to an interface. I. Exact-image theory formulation," J. Opt. Soc. Am. A **8**, 472–476 (1991).
7. I. V. Lindell and E. Alanen, "Exact image theory for the Sommerfeld half-space problem, part III: general formulation," IEEE Trans. Antennas Propag. **AP-32**, 1027–1032 (1984).
8. B. R. Johnson, "Light scattering from a spherical particle on a conducting plane: I. Normal incidence," J. Opt. Soc. Am. A **9**, 1341–1351 (1992).
9. T. C. Rao and R. Barakat, "Plane-wave scattering by a conducting cylinder partially embedded in a ground plane. I. TM case," J. Opt. Soc. Am. A **6**, 1270–1280 (1989).
10. F. Borghese, P. Denti, R. Saija, G. Toscano and O. I. Sindoni, "Multiple electromagnetic scattering from a cluster of spheres. I. Theory," Aerosol Sci. Technol. **3**, 227–235 (1984).
11. E. M. Rose, *Multipole fields*, (Wiley, New York, 1956), Chap. 2, p. 10–24.
12. E. M. Rose, *Elementary Theory of Angular Momentum*, (Wiley, New York, 1957), Chap. 4, p. 50; Chap. 5, p. 76 and p. 98–106.
13. R. G. Newton, *Scattering theory of waves and particles*(McGraw-Hill, New York, 1966), Chap. 1, p. 24–28; Chap. 2, p. 30–52.
14. J. D. Jackson, *Classical electrodynamics*, (Wiley, New York, 1975), Chap. 9, p. 453–459; Chap. 16, p. 739–775.
15. R. T. Wang, J. M. Greenberg and D. W. Schuerman, "Experimental results of the dependent light scattering by two spheres," Optics Lett. **11**, 543–545 (1981).
16. F. Borghese, P. Denti, R. Saija and O. I. Sindoni, "Reliability of the theoretical description of electromagnetic scattering from non-spherical particles", J. Aerosol Sci. **20**, 1079–1081 (1989).
17. F. Borghese, P. Denti, R. Saija, G. Toscano and O. I. Sindoni, "Macroscopic optical constants of a cloud of randomly oriented nonspherical scatterers," Nuovo Cim. B **81**, 29–50 (1984).
18. M. Hammermesh, *Group theory* (Addison-Wesley, Reading, Mass., 1962), Chap. 9, p.322.
19. P. C. Waterman: "Symmetry, unitarity and geometry in electromagnetic scattering," Phys. Rev. D **3**, 825–839 (1971).
20. F. Borghese, P. Denti, R. Saija, G. Toscano and O. I. Sindoni, "Multiple electromagnetic scattering from a cluster of spheres. II. Symmetrization," Aerosol Sci. Technol. **3**, 237–243 (1984).
21. F. Borghese, P. Denti, R. Saija, G. Toscano and O. I. Sindoni, "Use of group theory for the description of the electromagnetic scattering from molecular systems," J. Opt. Soc. Am. A **1**, 183–191 (1984).
22. R. Balescu, *Equilibrium and nonequilibrium statistical mechanics*, (Wiley, New York, 1975), sect. 8.1, p. 257–259.
23. H. C. van de Hulst, *Light scattering by small particles* (Dover, New York, 1981), Chap. 4, p. 31–32; Chap. 9, p. 114; Chap. 15, p.297; Chap. 16, p. 329.
24. F. Borghese, P. Denti, R. Saija, G. Toscano and O. I. Sindoni, "Optical absorption coefficient of a dispersion of clusters composed of a large number of spheres", Aerosol Sci. Technol. **6**, 173–181 (1987).
25. F. Borghese, P. Denti, G. Toscano and O. I. Sindoni, "An addition theorem for vector Helmholtz harmonics", J. Math. Phys. **21**, 2754–2755 (1980).

Fig. 1. Sketch of the arrangement that we chose for the display of our results. The reflecting surface coincides with the xz axis and the y axis points towards the accessible half-space whose refractive index is $n = 1$. The polar angles of the direction of observation range in the intervals $0° \leq \vartheta_s \leq 180°$ and $0° \leq \varphi_s \leq 180°$. The direction of incidence, $\hat{\mathbf{k}}_I$, that is indicated by the arrow, has the polar angles $\vartheta_I = 90°$ and $\varphi_I = 225°$. The arrangement of the four-hemispheres linear chain whose scattering pattern is reported in Fig. 2(d) below is also shown.

Fig. 2. Pattern of the scattered intensity (a) for a single sphere on the reflecting surface, (b) for a dispersion of randomly-oriented two-spheres clusters, (c) for a dispersion of randomly oriented four-hemispheres linear chains and (d) for a four-hemispheres linear chain oriented as shown in Fig. 1. The wavelength of the incident wave is $\lambda = 628.3\,\text{nm}$ and the refractive index of all the scatterers is $n_0 = 3$. The radius of the single sphere in (a) is $b_s = 126.0\,\text{nm}$ whereas the radius both of the spheres of the two-spheres cluster in (b) and of the hemispheres of the four-hemispheres linear chain in (c) and (d) is $b_h = 100\,\text{nm}$. We actually report (in square meters) the quantities $r^2 I_{\varphi_s\varphi_s}/I_0$ in (a) and (d) and $r^2\langle I_{\varphi_s\varphi_s}\rangle/I_0$ in (b) and (c) as a function of the angles of observation ϑ_s and φ_s. r^2 is the distance of observation, I_0 is the incident intensity, $I_{\varphi_s\varphi_s}$ is the observed intensity and $\langle I_{\varphi_s\varphi_s}\rangle$ the orientationally-averaged observed intensity.

Fig. 3. Pattern of the scattered intensity (a) for a single sphere, (b) for a dispersion of randomly oriented two-spheres clusters, (c) for a dispersion of randomly-oriented two-hemispheres clusters and (d) for a dispersion of randomly-oriented four-hemispheres linear chains. The radii and the refractive indices are as in Fig. 2; the radius of the hemispheres of the two-hemispheres cluster equals the radius of the single sphere. We report (in square meters) $r^2 I_{\varphi\vartheta}/I_0$ in (a) and $r^2\langle I_{\varphi\vartheta}\rangle/I_0$ in (b), (c) and (d).

Fig. 4. Same as Fig. 3 except that $r^2 I_{\vartheta_s\varphi_s}/I_0$ and $r^2\langle I_{\vartheta_s\varphi_s}\rangle/I_0$ are considered.

F. Borghese et. al.
"Opt. properties..."
Fig. 1

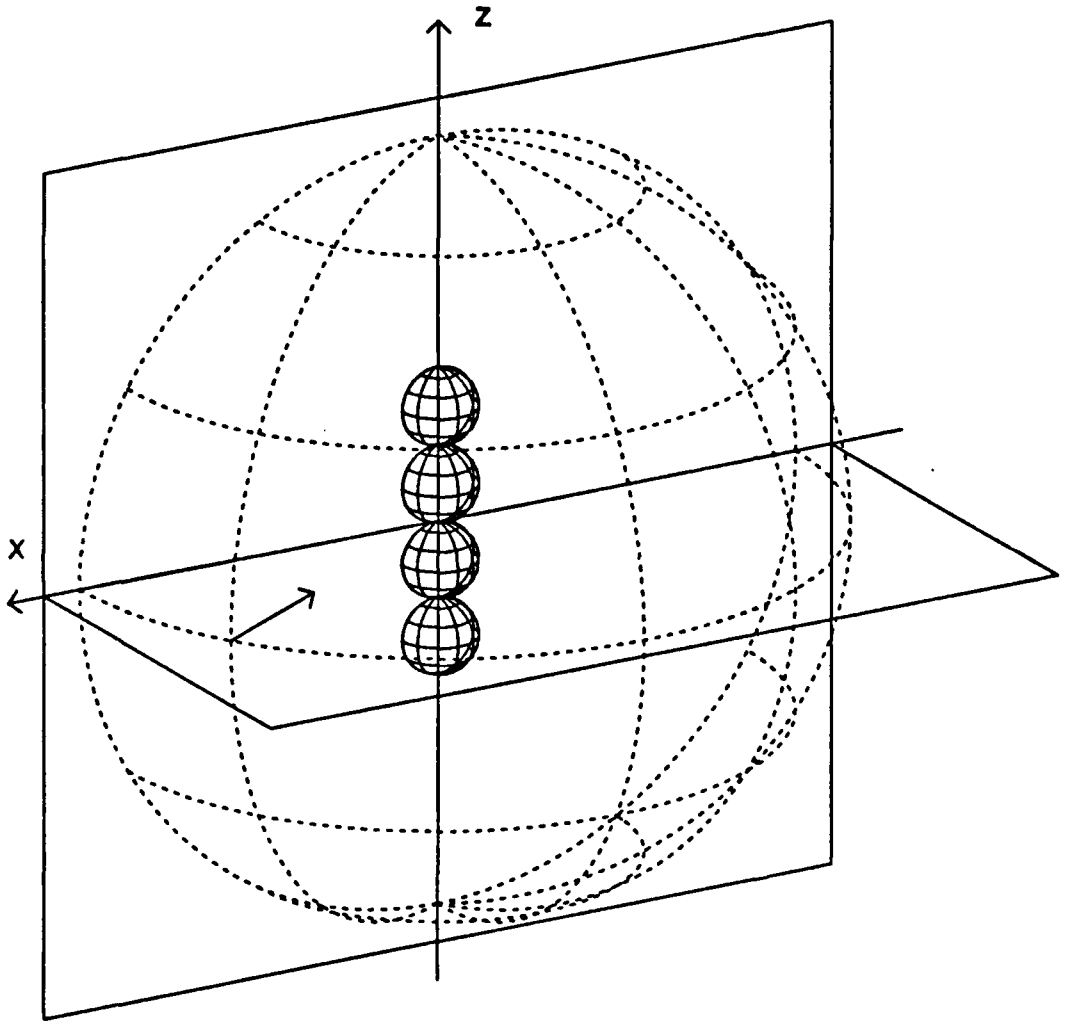

F. Borghese et al.
"Opt. properties"
Fig. 2a

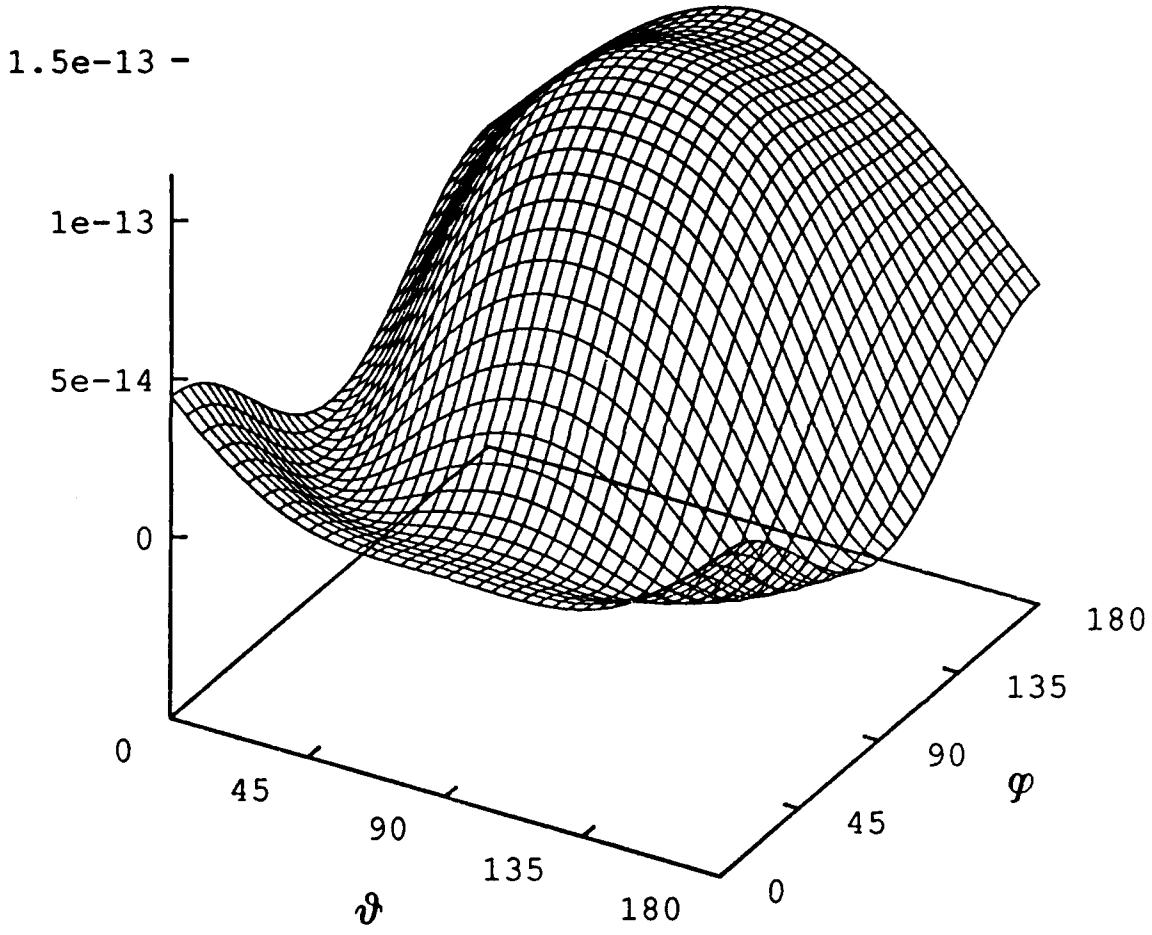

F. Borghese et al
"Opt. properties"
Fig. 2b

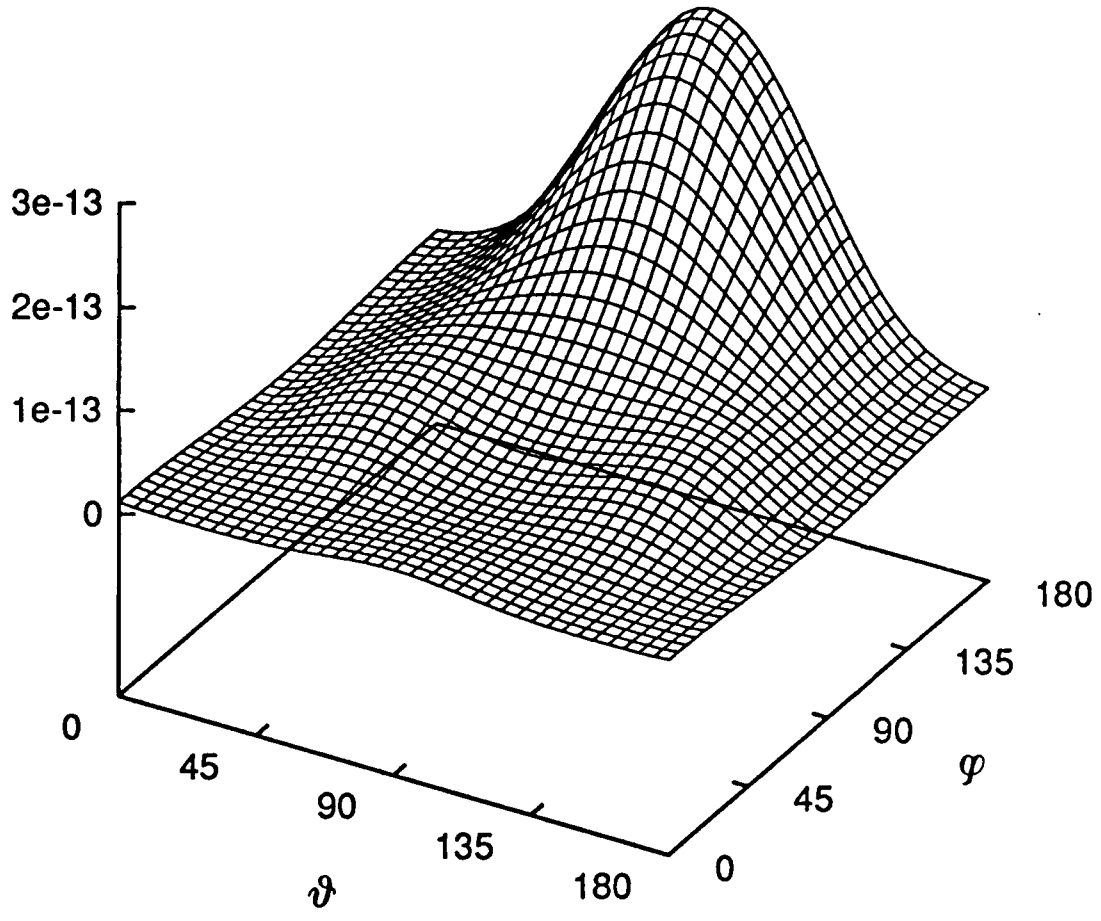

F. Borghese et al.
"Opt. properties"
Fig. 2c

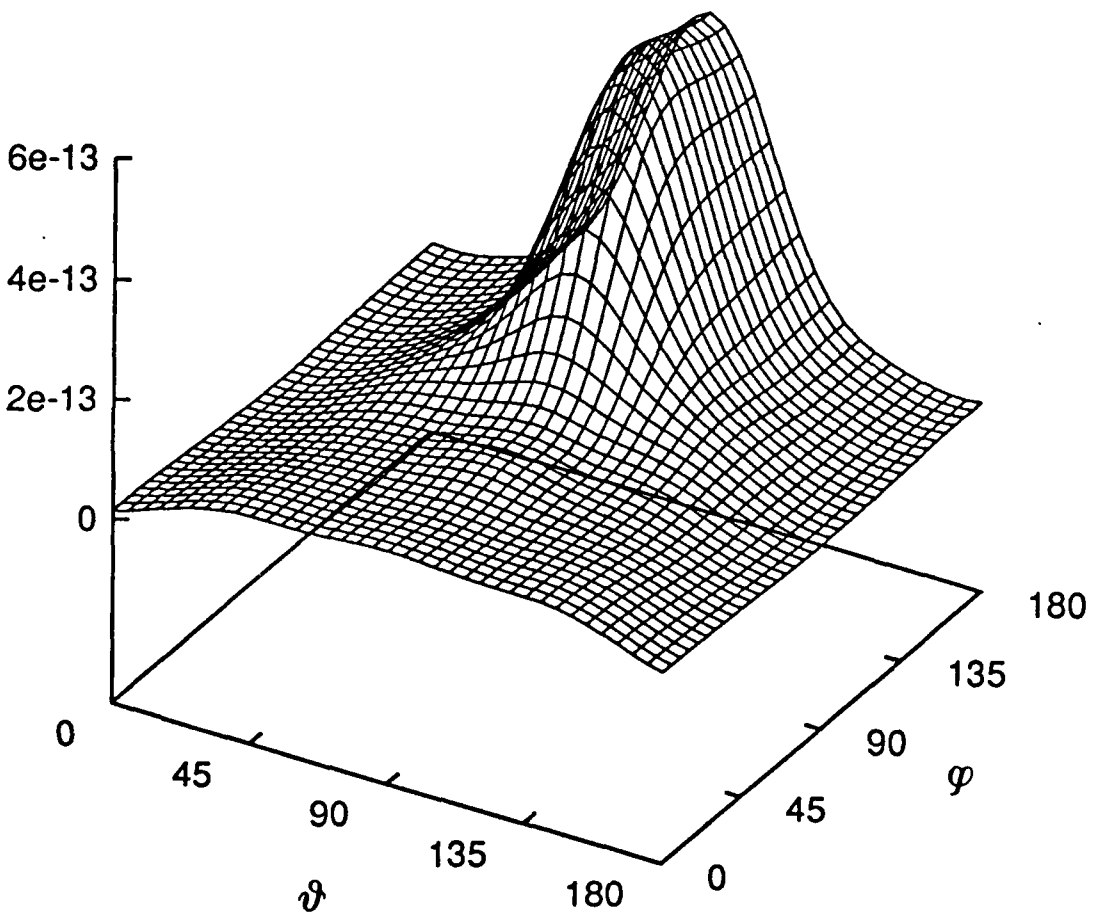

F. Borghese et al.
"Opt. properties"
Fig. 2d

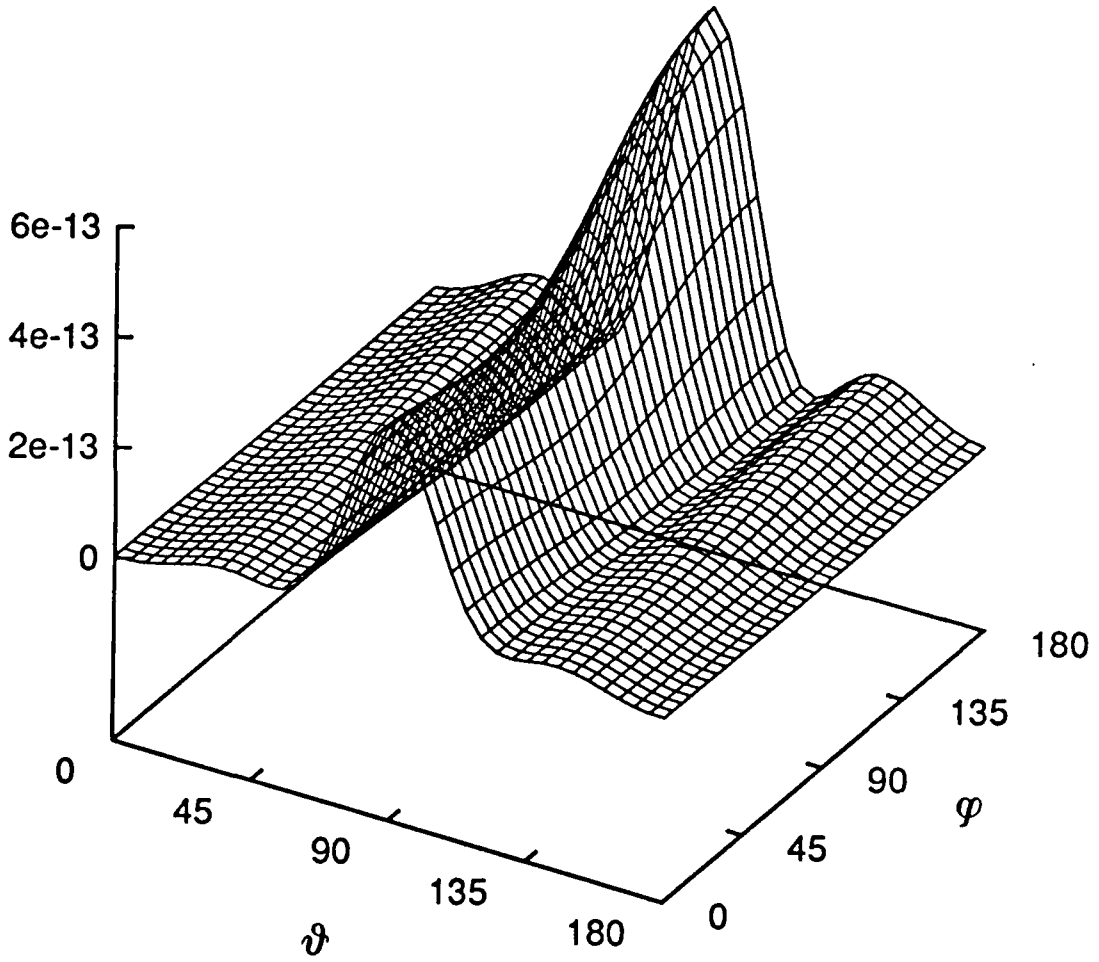

F. Borghese et al.
"Opt. properties..."
Fig. 3a

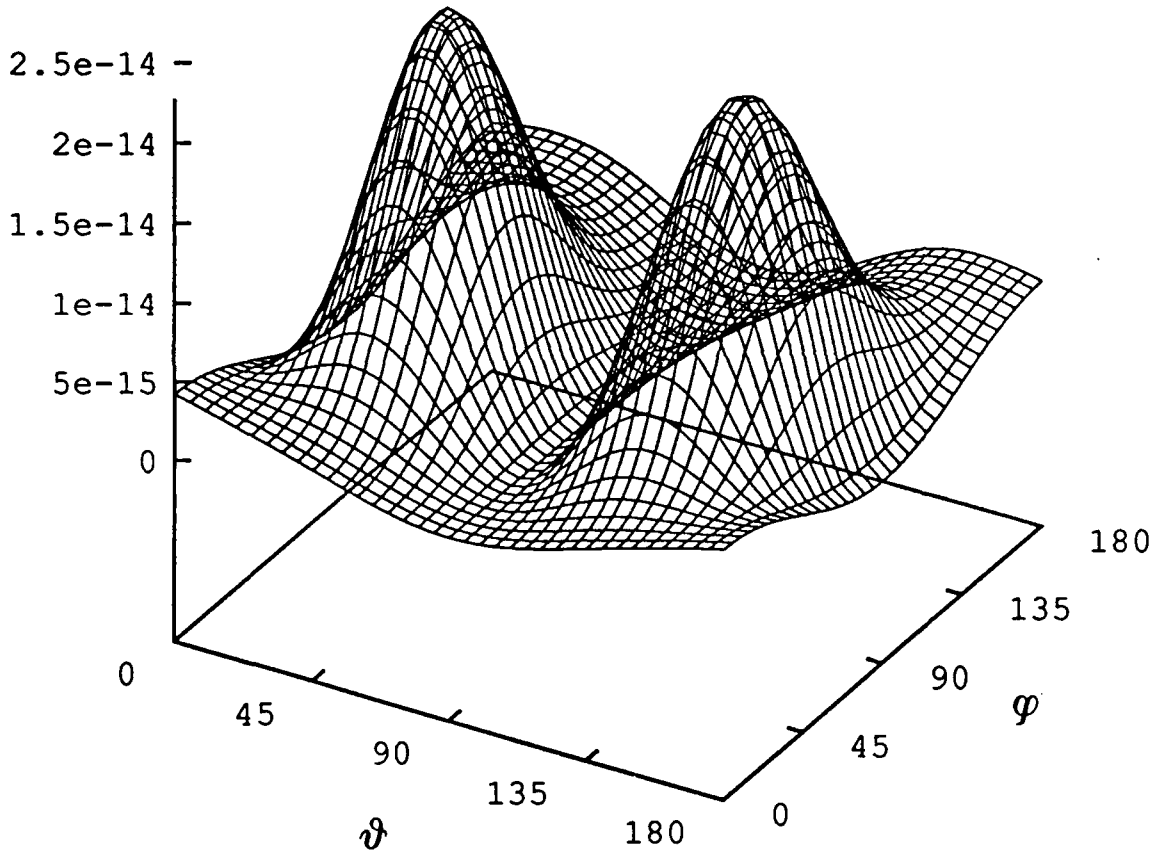

F. Borghese et al
"Opt. properties"
Fig. 3b

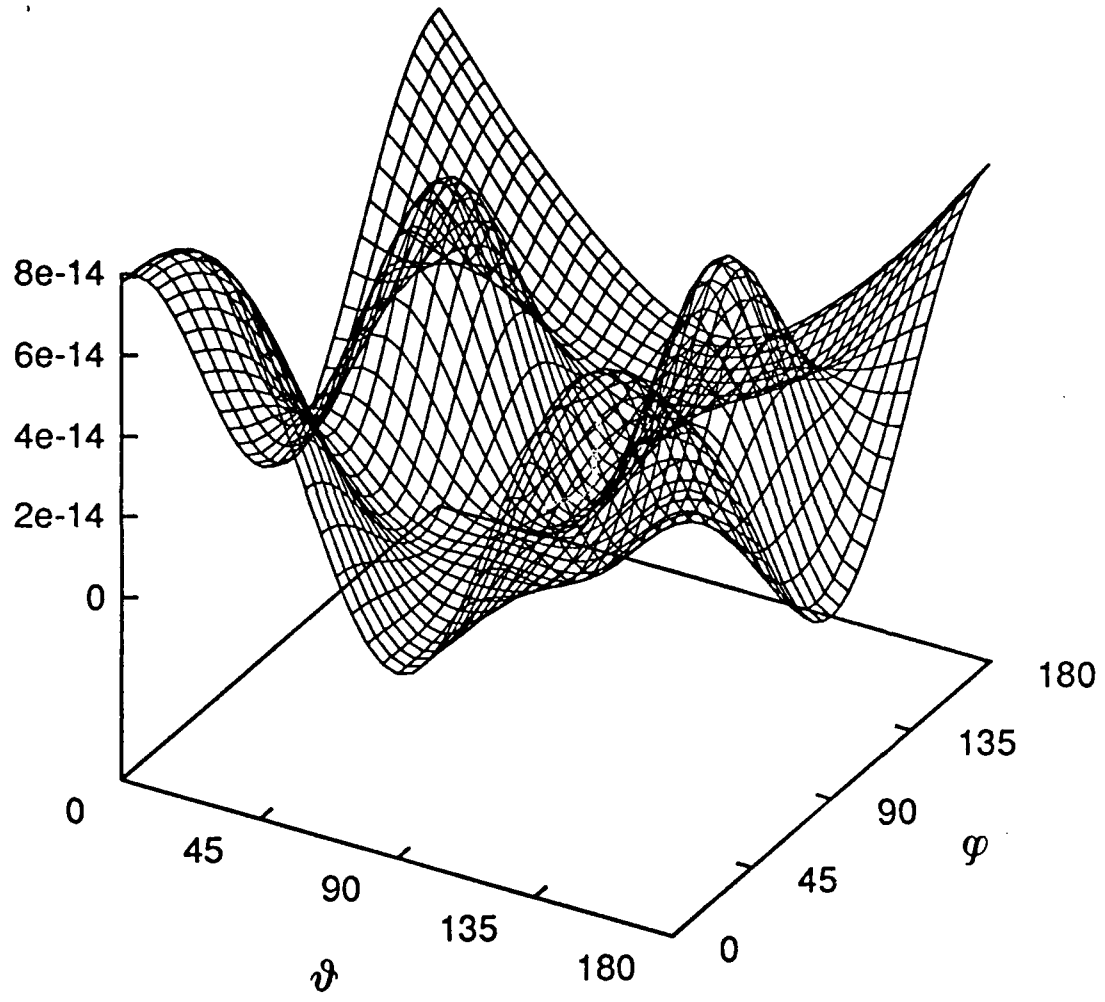

F. Borghese et al.
"Opt. properties"
Fig. 3c

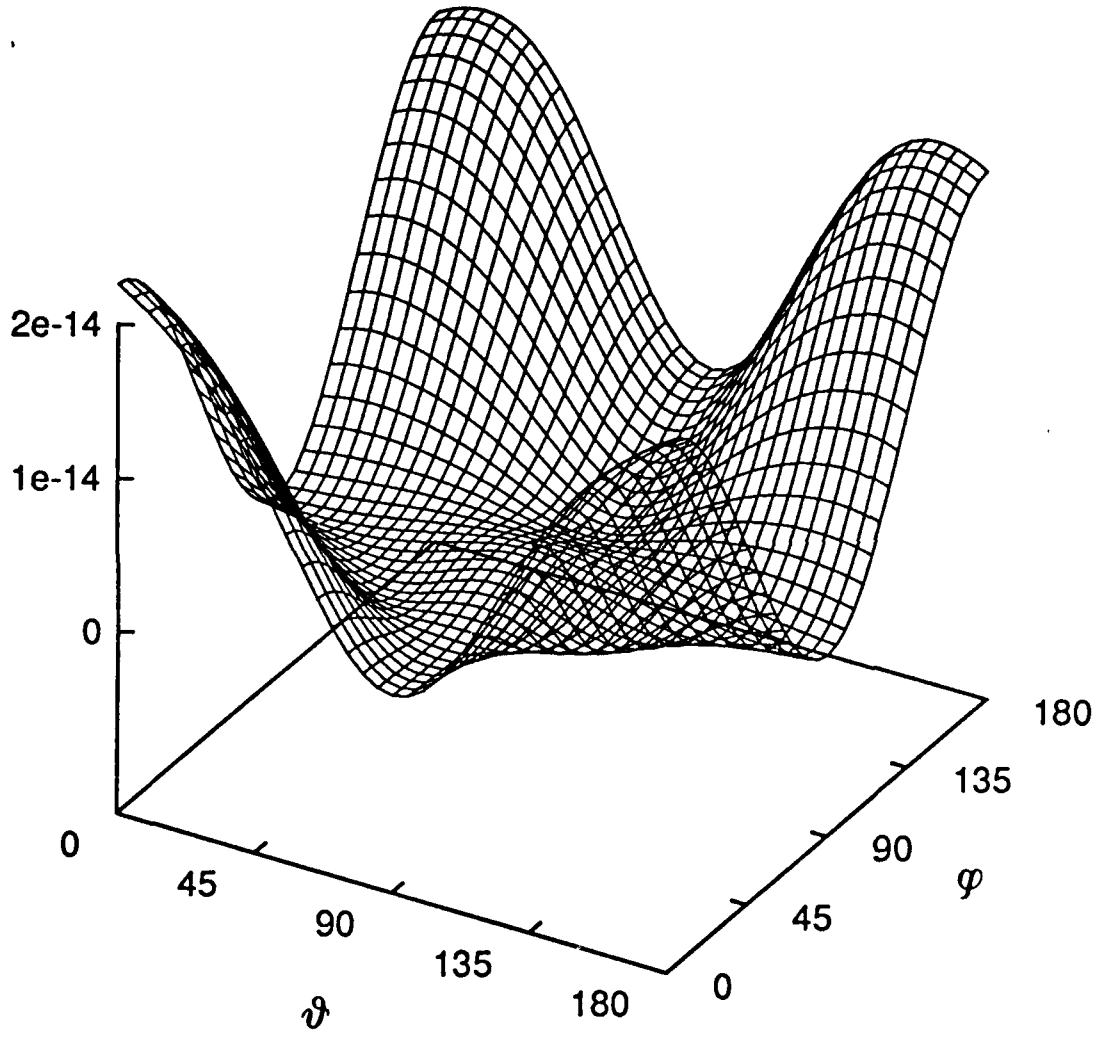

F. Borghese et. al.
"Opt. Properties"
Fig. 3d

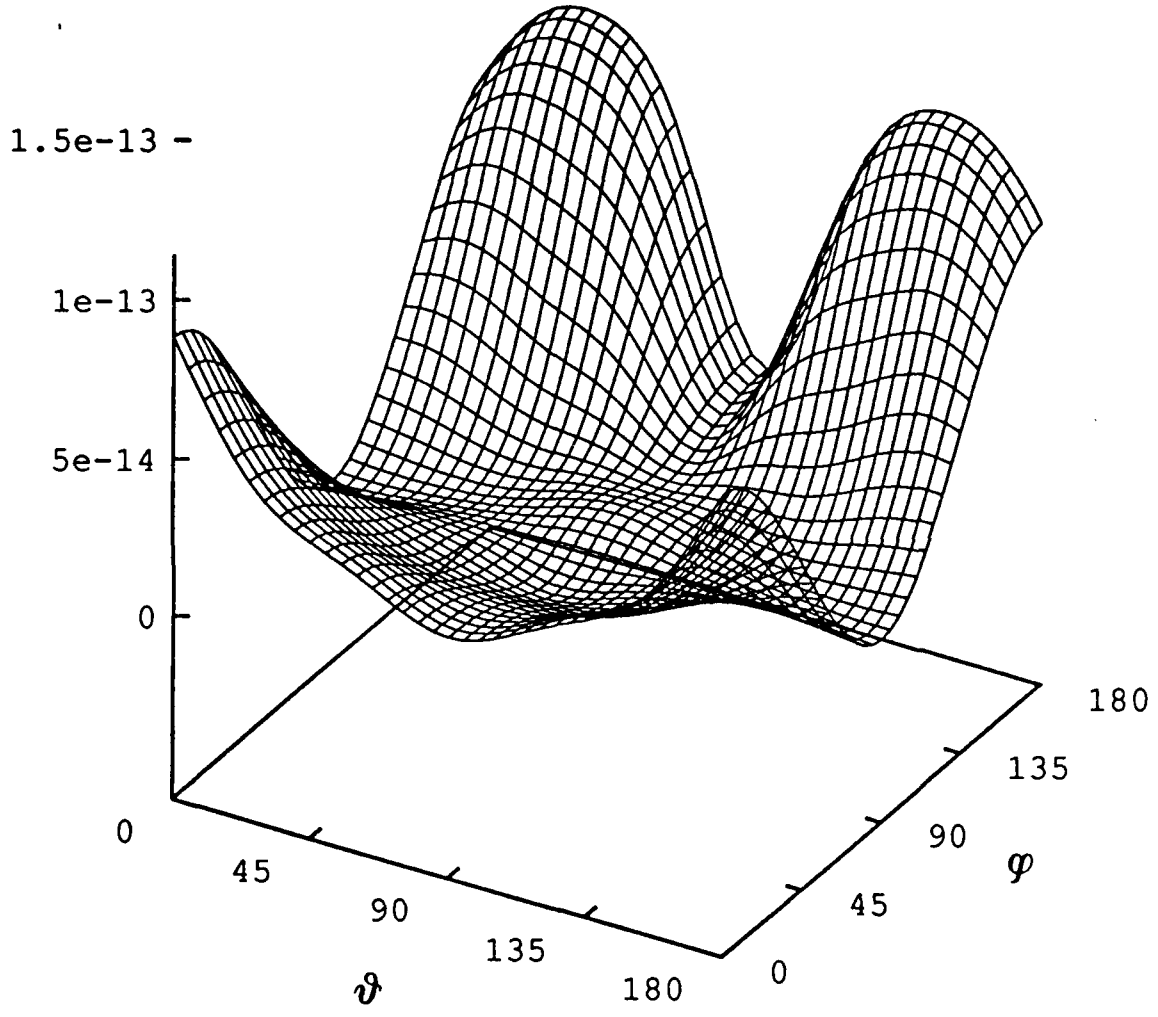

F. Borgrese et al.
"Opt. properties"
Fig. 4a

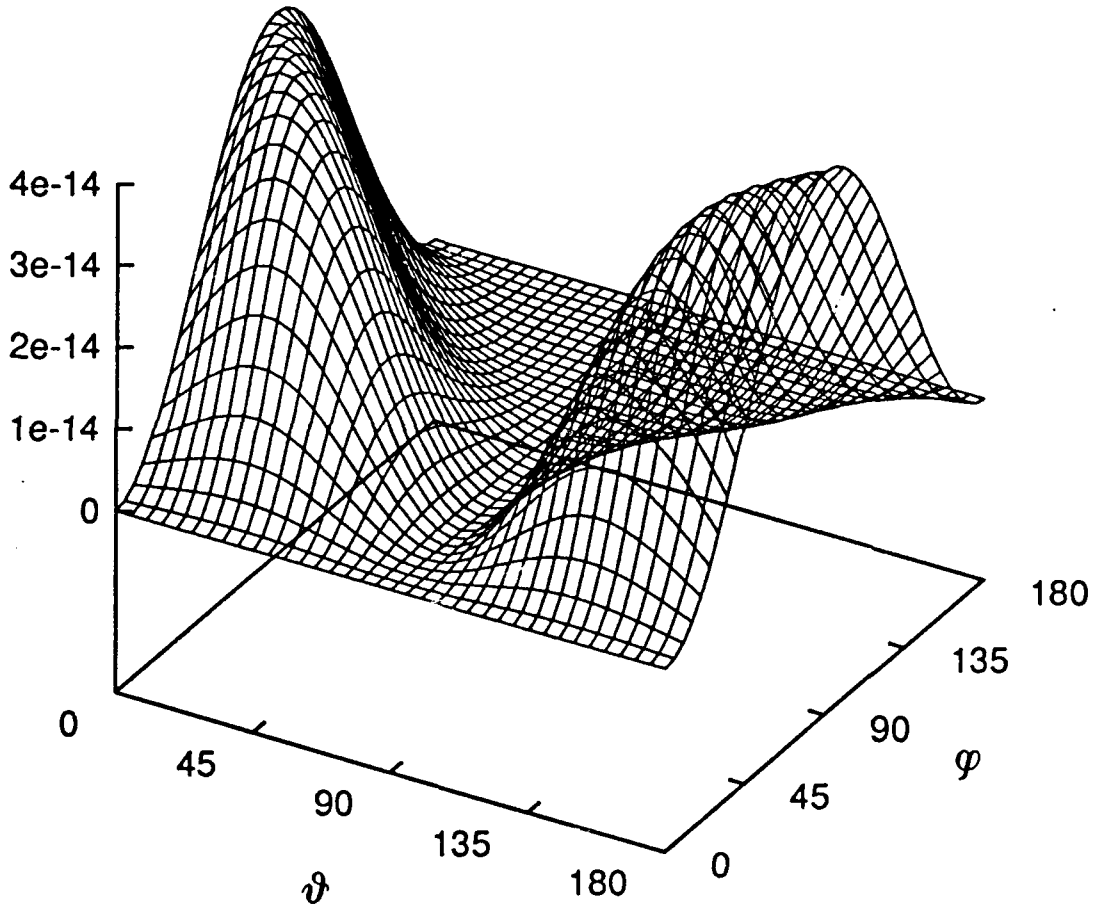

F. Borghese et al.
"Opt. properties"
Fig. 4b

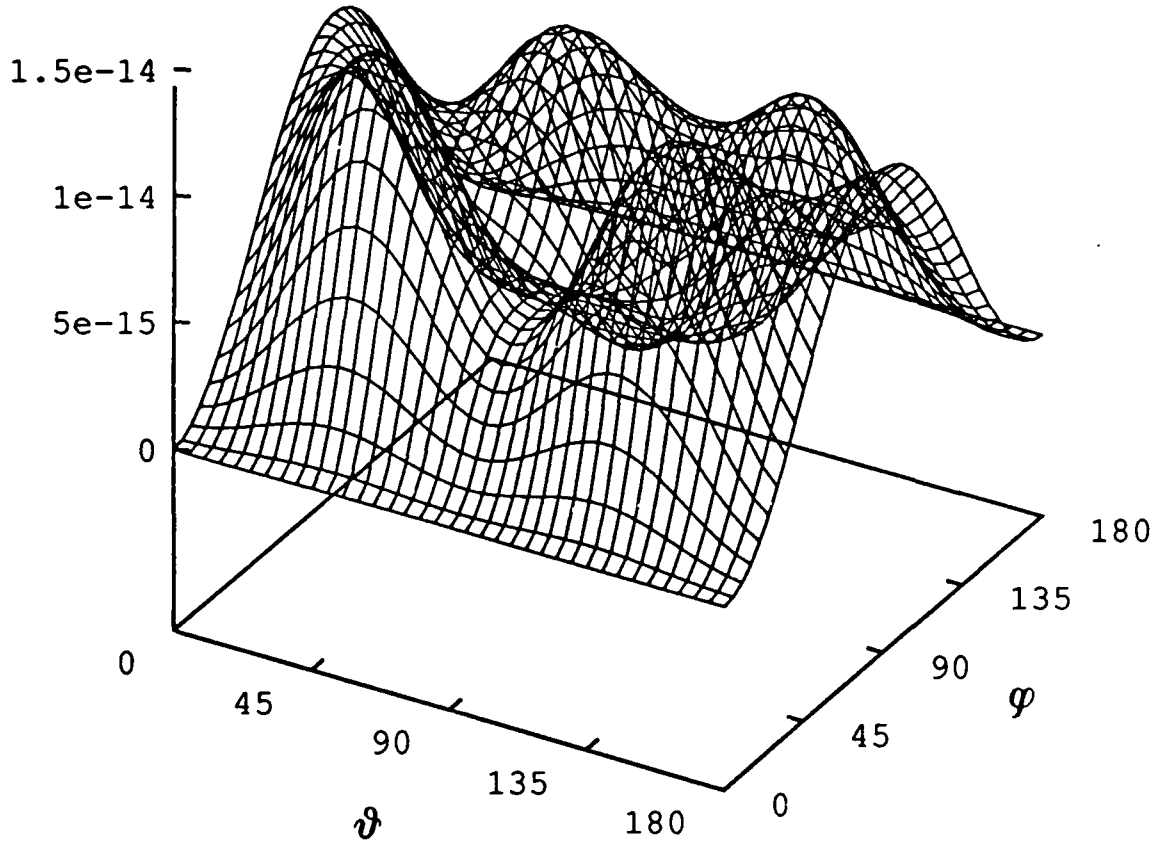

F. Borghese et al.
"Opt. properties..."
Fig. 4c

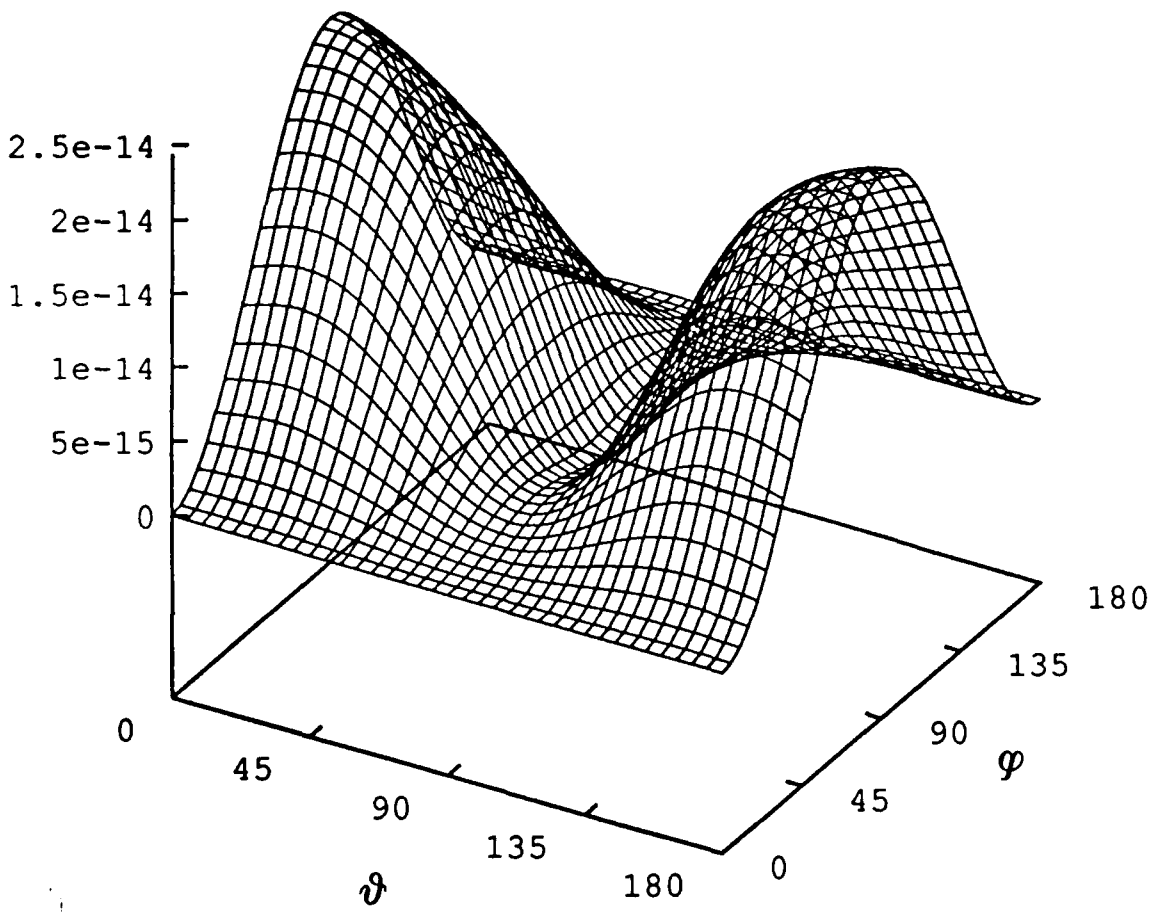

F. Borghese et al.
"Opt. properties"
Fig. 4d